

# Federated Survival Analysis with Discrete-Time Cox Models

Mathieu Andreux<sup>\*1§</sup>, Andre Manoel<sup>2†§</sup>, Romuald Menuet<sup>1§</sup>,  
Charlie Saillard<sup>1§</sup>, and Chloé Simpson<sup>3†§</sup>

<sup>1</sup>Owkin Inc., New York, USA.

<sup>2</sup>Hospital Israelita Albert Einstein, São Paulo, Brazil

<sup>3</sup>French Red Cross Innovation, Montrouge, France

June 17, 2020

## Abstract

Building machine learning models from decentralized datasets located in different centers with federated learning (FL) is a promising approach to circumvent local data scarcity while preserving privacy. However, the prominent Cox proportional hazards (PH) model, used for survival analysis, does not fit the FL framework, as its loss function is non-separable with respect to the samples. The naïve method to bypass this non-separability consists in calculating the losses per center, and minimizing their sum as an approximation of the true loss. We show that the resulting model may suffer from important performance loss in some adverse settings. Instead, we leverage the discrete-time extension of the Cox PH model to formulate survival analysis as a classification problem with a separable loss function. Using this approach, we train survival models using standard FL techniques on synthetic data, as well as real-world datasets from The Cancer Genome Atlas (TCGA), showing similar performance to a Cox PH model trained on aggregated data. Compared to previous works, the proposed method is more communication-efficient, more generic, and more amenable to using privacy-preserving techniques.

## 1 Introduction

The goal of survival analysis is to infer the occurrence time of some event for individuals, be it failure times in the case of industrial installations, or adverse events for patients in a clinical setting [15]. In the latter case, the resulting models, often based on the Cox proportional hazards (PH) model [8], are routinely used by clinicians for prognostic purposes and by biomedical researchers for understanding diseases, see *e.g.* [30] and [6] respectively.

One of the characteristics of clinical data is its relative global abundance, while being scarce in individual centers, especially for rare diseases. Aggregating local datasets is often impossible due to their sensitivity and strict privacy regulations. In this setting, federated learning [26, 19]

---

\*Corresponding author: [mathieu.andreux@owkin.com](mailto:mathieu.andreux@owkin.com).

†Work done while at Owkin.

§Alphabetical order.

is a promising approach as it enables collaboratively training models over multiple centers without moving the datasets.

This paper investigates the problem of training Cox PH survival models in this federated setting. This setting is challenging since the Cox PH loss function is not separable with respect to either centers or individual records, and therefore does not fit into existing frameworks for federated learning.

Among existing works tackling this problem, the WebDISCO algorithm [18] is the closest to our setting. While it permits one to train the Cox PH model on decentralized datasets, it has a large communication cost, is limited to linear models, and may expose some private data, as we show in Sec. 4. In this paper, we target a communication-efficient, generic, and privacy-preserving method for federated survival analysis.

## 1.1 Main contributions

1. We show that naïvely doing federated learning with the non-separable Cox loss leads to the so-called stratified Cox model, with per-center stratification (Sec. 3). Moreover, we demonstrate how, in extreme cases, this stratification might have severe consequences for the model’s predictive performance (Sec. 6.1).
2. We provide a workaround to this issue by approximating the Cox loss with a discrete-time model (Sec. 5) which, asymptotically, provides the same results as the original continuous-time model [32]. Since the loss for this model is separable, it can be easily plugged in existing federated learning algorithms. We empirically study the impact of this approximation in both synthetic and real-world tabular datasets (Sec. 6.1 and 6.2).
3. We use the proposed method to analyze multimodal datasets from The Cancer Genome Atlas (TCGA), which provide both image and tabular patient data along with survival statistics. We demonstrate the flexibility of our approach by combining it with deep learning models and training it on large whole-slide histopathology images (Sec. 6.3).

## 2 Background

### 2.1 Survival analysis

Given a group of individuals susceptible to experiencing an event of interest, survival analysis techniques seek to infer the probability distribution for the time of that event for each individual [15]. Such techniques are widely used in medical settings, *e.g.* for prognostic purposes, where individuals are patients and the event can be the onset of a disease, admission to a hospital, or death.

Obtaining these times-to-event requires patients to be followed in long observational studies, which typically last years. Due to this long duration, patients frequently drop out from studies before any event occurs. In this case, one can only know that the event did not occur before the dropping time, which is known. This partial knowledge is known in survival analysis as *right censoring*.

**Notation** We consider individuals  $i \in [N] = \{1, \dots, N\}$ , each represented by a tuple  $(\mathbf{x}_i, t_i, \delta_i)$ : a vector of covariates  $\mathbf{x}_i \in \mathbb{R}^P$ , an observed time point  $t_i \in \mathbb{R}_+$ , and an indicator of whether or

not an event occurred,  $\delta_i \in \{0, 1\}$ , where  $\delta_i = 0$  if the event has been censored. Due to censoring, the observed time  $t_i$  is only a lower-bound on the actual event time  $\tau_i \in \mathbb{R}_+$  for individual  $i$ ; these values match when  $\delta_i = 1$ .

The goal of survival analysis is to model the probability distribution of the random variable  $\tau_i$  for each individual  $i$ . A key quantity characterizing this distribution is the hazard function  $\lambda(t, \mathbf{x}_i)$ , which is the instantaneous rate of occurrence of the event given that it has not yet happened

$$\lambda(t, \mathbf{x}_i) = \lim_{\Delta t \rightarrow 0} \frac{\mathbb{P}[t \leq \tau_i \leq t + \Delta t | \mathbf{x}_i, \tau_i \geq t]}{\Delta t}. \quad (1)$$

**The Cox proportional hazards model** The Cox proportional hazards (PH) model [8] is one of the most used models in survival analysis. It assumes that the hazard function can be factored as

$$\lambda(t, \mathbf{x}_i) = \lambda_0(t) \exp(\boldsymbol{\beta}^T \mathbf{x}_i), \quad (2)$$

where  $\lambda_0(t)$  is the baseline hazard function—common to all individuals in the group and dependent on time only—and  $\boldsymbol{\beta}$  is the vector of parameters of the model. Notably, the model implies that the risk ratio between individuals does not depend on time. Therefore, when only interested in relative comparisons, the baseline hazard function does not need to be specified.

The function  $\lambda_0(t)$  and the parameters  $\boldsymbol{\beta}$  can be estimated independently from each other. For the latter, one can minimize the negative Cox partial log-likelihood, which only compares relative risk ratios and is defined by

$$\mathcal{L}(\boldsymbol{\beta}) = - \sum_{i: \delta_i=1} \left\{ \boldsymbol{\beta}^T \mathbf{x}_i - \log \sum_{j: t_j \geq t_i} e^{\boldsymbol{\beta}^T \mathbf{x}_j} \right\}. \quad (3)$$

Crucially, due to the log-sum-exp term in the r.h.s. of (3), which depends on a ranked subset of individuals, this partial log-likelihood cannot be written as a sum of terms depending each on a single  $\mathbf{x}_i$ . For that reason, we say that the Cox partial log-likelihood is *non-separable*.

**Stratification** The stratified Cox model [13] is a variation of the Cox PH model for a multi-center setting, in which each center can have a different baseline hazard function but the parameters  $\boldsymbol{\beta}$  are shared across centers. It can be useful if the suspicion exists that the PH assumption holds locally, but not globally. As noted by [12], the resulting stratified log-likelihood then reads as the sum of the per-center Cox log-likelihoods (3), *i.e.*

$$\mathcal{L}_{\text{strat}}(\boldsymbol{\beta}) = - \sum_{k=1}^C \sum_{\substack{i \in I_k \\ \delta_i=1}} \left\{ \boldsymbol{\beta}^T \mathbf{x}_i - \log \sum_{\substack{j \in I_k \\ t_j \geq t_i}} e^{\boldsymbol{\beta}^T \mathbf{x}_j} \right\}, \quad (4)$$

where  $C$  is the number of centers, indexed by  $k = 1, \dots, C$ , and  $I_1, \dots, I_C \subset [N]$  denote the partition of individuals across these centers. Crucially, the stratified Cox log-likelihood is separable at the center level, but not at the patient level.

**Discrete-time extension** When the number of individual times-to-event is small, be it after quantization or because of the data distribution, it is often profitable to take into account the discrete nature of the observations for modelling purposes [23].

In this case, let  $\{s^{(m)}\}_{m \in [T]}$  denote the ordered set of unique times-to-event of size  $T$ , such that  $s^{(1)} < \dots < s^{(T)}$ . The hazard function is thus defined as a weighted sum of Dirac functions  $\delta(t - s^{(m)})$  located at times  $s^{(m)}$ ,

$$\lambda(t, \mathbf{x}_i) = \sum_{m=1}^T p^{(m)}(\mathbf{x}_i) \delta(t - s^{(m)}), \quad (5)$$

where  $p^{(m)}(\mathbf{x}_i)$  is the conditional probability of individual  $i$  having an event at time  $s^{(m)}$ , knowing that the individual is still at risk at that time:

$$p^{(m)}(\mathbf{x}_i) = \mathbb{P}[\tau_i = s^{(m)} \mid \mathbf{x}_i, \tau_i \geq s^{(m)}]. \quad (6)$$

The Cox PH model (2) then does not apply, due to the hazard function being bounded in  $[0, 1]$ . [8] proposes to adapt it in the discrete-time setting as

$$\frac{p^{(m)}(\mathbf{x}_i)}{1 - p^{(m)}(\mathbf{x}_i)} = \frac{p_0^{(m)}}{1 - p_0^{(m)}} \exp(\boldsymbol{\beta}^T \mathbf{x}_i), \quad (7)$$

with  $\{p_0^{(m)}\}_{m \in [T]}$  leading to a baseline hazard function. Denoting the sigmoid function by  $\sigma(x) = (1 + e^{-x})^{-1}$  and introducing coefficients  $\alpha^{(m)} \triangleq \sigma^{-1}(p_0^{(m)})$ , (7) implies that the conditional survival probability follows a logistic model with time-dependent biases  $\alpha^{(m)}$  and time-independent weights  $\boldsymbol{\beta}$ :

$$p^{(m)}(\mathbf{x}_i) = \sigma(\alpha^{(m)} + \boldsymbol{\beta}^T \mathbf{x}_i). \quad (8)$$

Discrete-time models can be used as approximations to continuous-time ones. This is done in [32], where multiple classifiers with tied weights give the probability of patients still at risk to have an event at each given time. In particular, when logistic regression is used, (8) is recovered. [32] also introduce a stacking method to be able to cast this model as a standard classification model and train all its parameters at once; we employ the same approach in our proposed method (Sec. 5).

## 2.2 Federated learning

In federated learning (FL) [26, 19], one starts with data distributed among multiple centers and strives to jointly learn a predictive model from these data by transmitting as little information as possible from the centers. This can be accomplished in multiple ways, depending on the kind of model one is concerned with. For neural networks, trained *via* some variant of stochastic gradient descent (SGD), it is typically done by introducing a centralized *aggregator*, which will securely combine the gradients produced at each center.

Specifically, given multiple datasets  $Z_k = \{(\mathbf{x}_i, y_i)\}_{i \in I_k}$  for each center  $k \in [C]$ , a model  $f_\theta(\mathbf{x})$ , and a per-sample loss  $\ell(\hat{y}, y)$  between predictions  $\hat{y}$  and actual values  $y$ , we can write the per-sample *separable* loss with respect to model parameters  $\theta$  as

$$\mathcal{L}(\theta; \{Z_k\}_k) = \sum_{k=1}^C \sum_{i \in I_k} \ell(f_\theta(\mathbf{x}_i), y_i). \quad (9)$$

**Basic FL algorithm** A simple optimization algorithm to minimize this loss consists in a distributed minibatch stochastic gradient descent. At each optimization step  $q$ , each center  $k$  evaluates a local gradient  $g_{q,k}$  on some local batch  $B_{q,k} \subset I_k$  at the current shared value of the parameters  $\theta_q$ ,

$$g_{q,k} = \nabla_{\theta_q} \left[ \sum_{i \in B_{q,k}} \ell(f_{\theta_q}(\mathbf{x}_i), y_i) \right]. \quad (10)$$

These local gradients are then communicated to the aggregator, which computes an aggregated gradient  $\sum_{k=1}^C g_{q,k}$ . The aggregator iterates the optimization scheme to obtain new parameters  $\theta_{q+1}$ , which are communicated back to the centers.

It is possible to choose the local batches  $B_{q,k}$  to ensure that the above steps exactly match computations performed if the datasets were centralized. This can be done by first choosing a global batch  $B_q$  uniformly from  $\cup_k I_k = [N]$ , and then splitting it into multiple local batches  $B_{q,k} = B_q \cap I_k$ . Whenever we use this batch sampling scheme, we designate the resulting basic federated learning algorithm as *pooled-equivalent FL*.

Notice that the assumption that the loss is separable, at least by center, is key for federated learning, since communicating data points  $\mathbf{x}_i$  between centers is restricted. Some losses, and in particular the Cox loss (3), are not separable, and thus cannot be used straightforwardly in this framework.

**Improvements** A number of modifications can be done to improve the above formulation of FL. In particular, while it guarantees pooled performance is preserved, it also raises concerns regarding the amount of communication needed, as well as possible leakages of training data. To address the former, one might reduce the frequency of communications while doing more local steps, leading to a scheme called *federated averaging* [19]. This comes at the expense of having no guarantees on the convergence of the algorithm, which can be particularly problematic when data distribution significantly changes from center to center, *i.e.* when data is heterogeneous [31]. Another possibility is to make gradients sparse [25].

In order to prevent data leakages, techniques such as differential privacy [11, 2] and secure aggregation [3] can be used. From an empirical perspective, simply adding noise or sparsifying the gradients seems to be enough to prevent attacks seeking to recover data from gradients [33].

### 3 Motivation

Training a Cox PH model (2) in a federated fashion is challenging due to the non-separability of the Cox loss. Indeed, for estimating  $\beta$ , one needs to minimize the partial log-likelihood (3), where each term corresponding to individual  $i$  involves a sum over an index set of the form  $\{j | t_j \geq t_i\}$ . However, at the center  $k$  where  $i$  belongs, one does not have access to this full set, but only to its intersection with the local dataset  $I_k$ .

A possibility to circumvent this problem is to approximate the risk set  $\{j | t_j \geq t_i\}$  by its intersection with the local set  $I_k$ . However, this leads to a different model: if we are forced to stratify data by center, we are not minimizing the negative log-likelihood of the Cox PH model (3) but of a *stratified Cox model* (4). While using the stratified model might be desirable in some cases, it might also have severe consequences in terms of performance when the distributions of the different centers are not the same, as we show in Sec. 6.1.

As discussed in the next section, the distributed optimization of (3) is possible, but has a number of drawbacks. Instead, in Sec. 5, we propose working with a proxy to the Cox model, which has a separable loss and is thus amenable to federated learning in a plug-and-play fashion.

## 4 Previous Work

In [18], an algorithm named WebDISCO is introduced for training the Cox model (2) in a distributed fashion. In their approach, each center sends aggregate information to a central node for a number of rounds; the central node is then able to optimize the Cox partial log-likelihood as if all the data was pooled together. We now briefly review their method and expose its limitations.

**WebDISCO** For each center  $k$  and each unique event time  $s^{(m)}$ , we introduce  $D_k^{(m)}$  and  $R_k^{(m)}$  as the subsets of individuals in center  $k$  who had an event, and who are still at risk at time  $s^{(m)}$  respectively:

$$D_k^{(m)} \triangleq \left\{ i \in I_k \mid t_i = s^{(m)}, \delta_i = 1 \right\}, \quad (11)$$

$$R_k^{(m)} \triangleq \left\{ i \in I_k \mid t_i \geq s^{(m)} \right\}. \quad (12)$$

In order for the central server to compute the gradient of the Cox partial log-likelihood (3), each center  $k$  communicates to the central server the couple

$$\begin{cases} \zeta(R_k^{(m)}, \boldsymbol{\beta}) = \sum_{i \in R_k^{(m)}} \exp(\boldsymbol{\beta}^T \mathbf{x}_i), \\ \boldsymbol{\mu}(R_k^{(m)}, \boldsymbol{\beta}) = \sum_{i \in R_k^{(m)}} \mathbf{x}_i \exp(\boldsymbol{\beta}^T \mathbf{x}_i), \end{cases} \quad (13)$$

for all time indices  $m \in [T]$ . The gradient of the Cox partial log-likelihood (3) can then be computed as

$$\nabla_{\boldsymbol{\beta}} \mathcal{L}(\boldsymbol{\beta}) = \sum_{k=1}^C \sum_{m=1}^T \sum_{i \in D_k^{(m)}} \mathbf{x}_i - \sum_{m=1}^T \left( \sum_{k=1}^C |D_k^{(m)}| \right) \frac{\sum_{k=1}^C \boldsymbol{\mu}(R_k^{(m)}, \boldsymbol{\beta})}{\sum_{k=1}^C \zeta(R_k^{(m)}, \boldsymbol{\beta})}. \quad (14)$$

Analogous formulas are derived to allow the central server to build the Hessian thanks to quantities communicated by each center.

**Limitations** Compared to our work, WebDISCO is limited in the following aspects. In terms of bandwidth requirements, each center has to send, at each optimization step,  $\mathcal{O}(TP)$  terms for the gradients, and an additional  $\mathcal{O}(TP^2)$  for the Hessian if a second-order gradient descent is carried out, whereas our method only requires the exchange of  $\mathcal{O}(T + P)$  terms at each communication step. In terms of generality, the scope of the algorithm is limited to the linear Cox model; it cannot be adapted, for instance, to neural networks, which is the case for our method. In terms of privacy, it might leak sensitive information, as we detail in the next paragraph.

**Privacy leakage** In WebDISCO, the aggregate information that is sent by each center can reveal individual-level data. Notice that, by telescoping the communicated quantities with respect to  $m$ , the central server can infer  $\zeta(D_k^{(m)}, \boldsymbol{\beta})$  and  $\boldsymbol{\mu}(D_k^{(m)}, \boldsymbol{\beta})$ , which are aggregated measurements over a potentially much smaller set  $D_k^{(m)}$ , consisting only of patients who had an event at the given time.

If one such set  $D_k^{(m)}$  contains only one event, then the measurements of the related individual  $\mathbf{x}_i$  are exposed to the server. Indeed, in this case, the fraction  $\boldsymbol{\mu}(D_k^{(m)}, \boldsymbol{\beta}) / \zeta(D_k^{(m)}, \boldsymbol{\beta})$  is equal to  $\mathbf{x}_i$ .

If no such set contains a single element, the measurements of the related individuals are still at risk. Indeed, because an iterative optimization is carried out, the central server observes  $(\zeta(D_k^{(m)}, \boldsymbol{\beta}), \boldsymbol{\mu}(D_k^{(m)}, \boldsymbol{\beta}))$  for multiple measurements of  $\boldsymbol{\beta}$ . This can be seen as a system of nonlinear equations where the unknowns are the  $\{\mathbf{x}_i\}_{i \in D_k^{(m)}}$ , and for which numerical solutions can be attempted.

**Related survival models** Survival analysis is not confined to CoxPH models: other popular survival models include accelerated failure time (AFT) methods [29, 22] or non-parametric sampling-based methods [4, 20]. In the following, we focus on the CoxPH model as it is one of the most popular survival models, especially in the medical field [27, 28].

## 5 Methods

### 5.1 Discrete-time extended stacked Cox model

**Discrete-time setting** In the following, we consider the discrete-time approach introduced in Sec. 2.1. All observed times  $\{t_i\}_{i \in [N]}$  are binned to a finite set  $\{s^{(m)}\}_{m \in [T]}$  of size  $T$ . Note that this finite set may contain less values than the number of unique event times if the latter are first quantized. Such a quantization is performed by first choosing a binning interval  $Q$  and applying the mapping  $t \mapsto Q \lceil t/Q \rceil$  to observed times  $t_i$ .

**Extended Cox model** Given parameters  $\boldsymbol{\alpha} = (\alpha^{(1)}, \dots, \alpha^{(T)})$ ,  $\boldsymbol{\beta} \in \mathbb{R}^{P'}$  and a mapping  $\phi_\theta : \mathbb{R}^P \rightarrow \mathbb{R}^{P'}$  parametrized by  $\theta$ , we model the conditional probability of an event occurring at time  $s^{(m)}$  for individual  $i$  by

$$\begin{aligned} p_{\boldsymbol{\alpha}, \boldsymbol{\beta}, \theta}^{(m)}(\mathbf{x}_i) &= \mathbb{P}[\tau_i = s^{(m)} | \tau_i \geq s^{(m)}] \\ &= \sigma(\boldsymbol{\alpha}^{(m)} + \boldsymbol{\beta}^T \phi_\theta(\mathbf{x}_i)). \end{aligned} \quad (15)$$

This model is a *discrete-time proportional hazards* model which extends the Cox model (7) with an intermediate representation  $\phi_\theta(\mathbf{x}_i)$ . When  $\phi_\theta(\mathbf{x}_i) = \mathbf{x}_i$ , one retrieves the discrete-time Cox model. In general, however, one can employ more complex models such as neural networks.

**Stacking method** A simple method recasting (15) as a classification problem can be used to learn all the time-varying biases  $\boldsymbol{\alpha}$  at once [32]. For each sample  $(\mathbf{x}_i, t_i)$ , we first introduce the binary labels

$$y_i^{(m)} = \begin{cases} 0 & \text{if } t_i > s^{(m)} \\ \delta_i & \text{if } t_i = s^{(m)}, \end{cases} \quad (16)$$

for all  $m$  such that  $s^{(m)} < t_i$  and additionally, if  $\delta_i = 1$ , for  $m$  such that  $t_i = s^{(m)}$ . Notice that by construction  $\mathbb{P}[y_i^{(m)} = 1] = \mathbb{P}[\tau_i = s^{(m)} | \tau_i \geq s^{(m)}]$ .

For each original sample, we generate new samples

$$\mathbf{x}_i^{(m)} = \left[ \mathbf{e}^{(m)}, \mathbf{x}_i \right], \quad (17)$$

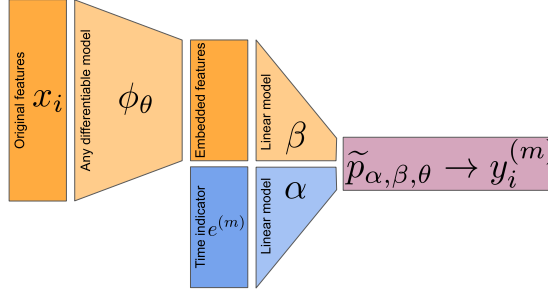


Figure 1: Parametric model  $\tilde{p}_{\alpha, \beta, \theta}(x_i^{(m)})$  to represent survival probabilities using the stacking method described by (18).

where  $e^{(m)} \in \mathbb{R}^T$  is the  $m$ -th vector of the canonical basis in dimension  $T$ . Each of the samples  $x_i^{(m)}$  is associated to label  $y_i^{(m)}$ .

The classification task associated to the *stacked* dataset  $\{(x_i^{(m)}, y_i^{(m)})\}_{i,m}$  corresponds to the occurrence of an event at the time encoded in the canonical vector, provided no event occurred at previous times. As a consequence, if we define a binary classification model on the stacked dataset as

$$\begin{aligned} \tilde{p}_{\alpha, \beta, \theta}(x_i^{(m)}) &= \sigma([\alpha; \beta]^T[e^{(m)}; \phi_\theta(x_i)]) \\ &= \mathbb{P}[y_i^{(m)} = 1], \end{aligned} \quad (18)$$

where  $[\cdot; \cdot]$  denotes vector concatenation, then this model satisfies

$$p_{\alpha, \beta, \theta}^{(m)}(x_i) = \tilde{p}_{\alpha, \beta, \theta}(x_i^{(m)}). \quad (19)$$

In other words, fitting (18) is equivalent to fitting (15). Model (18) is sketched in Fig. 1.

**Loss function** Thanks to the stacking method, the model parameters  $(\alpha, \beta, \theta)$  can be found by training model (18) on the stacked dataset with a standard classification loss. More precisely, we minimize the binary cross-entropy loss between the model  $\tilde{p}_{\alpha, \beta, \theta}(x_i^{(m)})$  and the true labels  $y_i^{(m)}$ ,

$$\mathcal{L}_{\text{BCE}}(\{\alpha, \beta, \theta\}; \{x_i^{(m)}, y_i^{(m)}\}_{i,m}) = \sum_{i=1}^n \sum_{\substack{m \\ t_i \geq s^{(m)}}} \ell_{\text{BCE}}(\tilde{p}_{\alpha, \beta, \theta}(x_i^{(m)}), y_i^{(m)}), \quad (20)$$

where  $\ell_{\text{BCE}}(\hat{y}, y) = -y \log \hat{y} - (1 - y) \log (1 - \hat{y})$ . This loss function can be easily and efficiently implemented in generic deep learning frameworks, opening the possibility of using advanced deep learning architectures for the intermediate representation  $\phi_\theta$ .

## 5.2 Federated learning

We now discuss the properties of the proposed model in the federated setting.

**Federated optimization** An important property of our loss (20) is that it is separable with respect to individual *stacked* samples. As a consequence, once the local stacked datasets have been built, it is straightforward to optimize our proposed model using the federated learning approach described in Sec. 2.2.

**Stacking in the federated setting** Prior to the federated optimization, each center needs to build the stacked datasets. Each center can do it individually provided the unique times  $s^{(m)}$  are known. As a consequence, all centers must first agree on the set  $\{s^{(m)}\}_{m \in [T]}$  of unique times.

Such an agreement can be reached easily since we use quantized times with a sampling period  $Q$ , as discussed in Sec. 5.1. Given  $Q$ , it is sufficient to compute the maximum event time among all centers for all individual centers to define a common grid. A maximum event time can be found by computing the maximum of all the local maxima. This computation can be performed either through the server or *via* multi-party computation [16], thereby ensuring privacy of the local event times.

**Computation and communication costs** At each communication round of a given federated learning algorithm, all the parameters need to be exchanged, which scales as  $\mathcal{O}(T + P' + |\theta|)$ . When no intermediate representation is used, this is equal to  $\mathcal{O}(T + P)$ , which is much lower than the  $\mathcal{O}(TP)$  required in the previously proposed WebDISCO algorithm.

In terms of computation costs, the stacking approach increases the number of samples, which is now upper-bounded by  $NT$  instead of the original  $N$ . Therefore, one has interest in choosing the sampling period  $Q$  such that  $T$  is small to prevent detrimental effects on the total computation time.

**Privacy** Although the stacked datasets can be built in a privacy-preserving fashion, the updates sent by the centers can leak information about their local datasets, as well as the central model. This is where the separability of the proposed model provides an important advantage: generic privacy-preserving methods for federated learning can be readily used for our model. For WebDISCO, on the other hand, further reflection is needed before applying generic privacy-preserving solutions such as differential privacy.

### 5.3 Learning schemes

In our experiments, we compare the performance of different learning schemes on multiple datasets. A scheme consists in both a model and a procedure for training it.

**Baselines** Our baselines consist in training the Cox model (2) in a non-distributed fashion. In particular, we evaluate i) the *pooled* performance (**POOL**), that of the model trained with all data pooled together; ii) the average *local* performance (**LOCAL**), that of the models trained at each center separately; and iii) the *ensembled* performance (**ENS**), that obtained by averaging the predictions of the models trained at each center. These models are trained using the **lifelines** library [9] implementation of the Newton method. We stress that, in terms of c-index, the **POOL** method is equivalent to the baseline WebDisco method [18].

Another baseline, which is used in Sec. 6.2, comes from training on pooled data, but using a *boosting* approach instead, specifically XGBoost [5] with the Cox partial log-likelihood as the objective function. In our experience, boosting typically gives similar or better results than linear methods in this context, and as such we use it as baseline when working with the TCGA datasets.

**Cox in minibatches (MINI)** This method consists in the optimization of the Cox loss (3) by means of minibatch SGD, or more generally a variant such as Adam. Notice that the risk set for

each individual is built by only considering samples present in the batch, but that each batch is sampled from the pooled data.

**Stratified/naïvely-federated Cox (N-FL)** Optimization of the Cox loss stratified by center (4). This is done following the procedure in Sec. 2.2, *i.e.* by combining gradients coming from the different centers. Risk sets are thus built considering only samples present in the batch *and* coming from the same center as the individual. We denote this scheme *naïve FL* in our experiments.

**Model (18) with pooled-equivalent FL (DT-FL)** We simulate this optimization of the loss (20) being done on separate centers with minibatches. However, since the loss is separable, one should obtain the same results if data is pooled together, see discussion in Sec. 2.2. For  $\phi_\theta$ , we choose either the identity function, in which case the discrete-time Cox model is recovered (Sec. 6.1 and 6.2), or a more complex neural network adapted to the task in hand (Sec. 6.3). We denote this scheme *discrete-time FL* in our experiments.

## 5.4 Performance evaluation

We evaluate the performance of each scheme by using cross-validation (CV) in two different ways. In the first, each center splits their data in 5 folds, and at the  $i$ -th round of the CV, all the  $i$ -th folds are combined together in order to build the test set. This procedure provides a proxy to how the model generalizes at the different centers, on average. As this computation might not be feasible in practice, we also study the *out-of-center* (OOC) generalization, by setting aside, at each round of CV, all data points of a given center.

The metric used to evaluate the models is the concordance index

$$\text{c-index} = \mathbb{E}_{\substack{i:\delta_i=1 \\ j:t_j>t_i}} \mathbb{1}_{[\eta_j < \eta_i]}, \quad (21)$$

where  $\eta_i$  is a risk score assigned to each individual—a high concordance index implies that risk scores and times-to-event are inversely ranked. For proportional hazards models, one can use as score the time-independent part of the hazard function. Thus, for the Cox models (2) and (8),  $\eta_i = \beta^T \mathbf{x}_i$ , and, for model (18),  $\eta_i = \beta^T \phi_\theta(\mathbf{x}_i)$ .

## 6 Results and Discussion

### 6.1 Experiments on synthetic tabular data

We start by showing the effects of the different schemes on synthetically-generated data. The features for each individual are generated by sampling from a normal distribution with variance  $1/P$ ,  $\mathbf{x}^{(i)} \sim \mathcal{N}(0, P^{-1}I_P)$ , thereby ensuring that  $\mathbb{E}\|\mathbf{x}^i\|^2 = 1$ . Observed times  $t_i$  are then set according to the following procedure. We first sample *actual times*  $\tau_i$  from a Cox model with constant baseline hazard, so that its c.d.f. is given by  $\Psi(u) \triangleq \mathbb{P}[\tau < u] = 1 - e^{-u \exp(\beta^T \mathbf{x}_i)}$ ; *censoring times* are then sampled from an uniform distribution  $U(0, \Psi^{-1}(\frac{1}{2}))$ . Finally, the observed times are defined as the minimum of censoring and actual times.

For this example, we simulate data distributed across  $C = 5$  centers with  $n = 1000$  patients each, where each patient is described by  $P = 200$  features. Experiments are performed either with

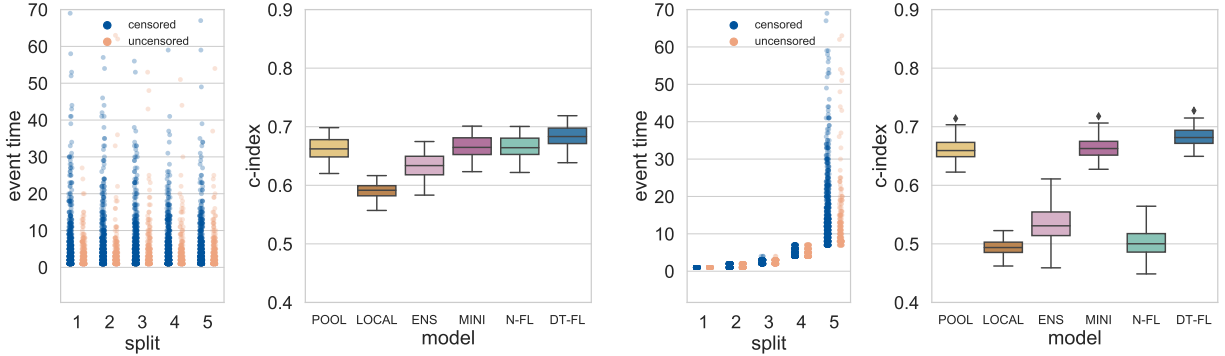


Figure 2: Experiments on synthetic data for learning schemes described in Sec. 5.3, generated according to the procedure described in Sec. 6.1. *Left*: performance of different schemes given synthetic data which is uniformly distributed across centers. Distribution of splits can be seen on the left. *Right*: analogous to the left figure, but given synthetic data ordered according to endpoint. Naïve federated scheme performance decreases considerably in this case, whereas discrete-time federated is not significantly affected.

data being uniformly distributed across centers, or stratified according to endpoint, see Fig. 2. We only perform 5-fold cross validation, as in the uniform case average and OOC performances are the same, and in the stratified case there is almost no OOC generalization. Displayed results are averages over 20 runs of 5-fold CV. Experimental details are provided in App. C.

We split the data across centers in two different ways. For the first experiment, we generate  $N = Cn$  samples according to the above procedure and then split them at random, assigning  $n$  of them to each center. As seen in Fig. 2, left, all methods perform similarly, apart from local and ensemble which, as expected, give subpar results. Note that as the underlying Cox models for the pooled and discrete-time FL methods differ, we do not expect their results to be exactly equal.

As a second experiment (Fig. 2, right), we order the samples per time of event  $t_i$  before splitting them, so that the smallest  $t_i$  go to the first center and the largest to the last. Doing this effectively destroys the performance of the naïve FL procedure, which minimizes the stratified loss (4). Most importantly, the performance of discrete-time FL remains unaltered—indeed, *it is not dependent on how the data is split across centers*. This is one of the main advantages of our approach.

## 6.2 Experiments on TCGA tabular datasets

For the experiments on real-world data, we use datasets from The Cancer Genome Atlas (TCGA). For each type of cancer with more than 200 patients, we download clinical information and preprocess datasets separately, transforming the categorical variables into dummy variables and removing columns with more than 95% of missing values. We use the curated TCGA Pan-Cancer Clinical Data Resource (TCGA-CDR) [17] to obtain the overall survival time and event status for each patient.

We first train baseline boosting models described in Sec. 5.3 on the generated features and labels, and keep the four cancer types with the highest average score obtained in 50 cross-validation runs. The four selected cancer types are: Breast Invasive Carcinoma (BRCA), Colon Adenocarcinoma (COAD), Kidney Renal Clear Cell Carcinoma (KIRC), and Low Grade Glioma (LGG). Details can be found in Tab. 1.

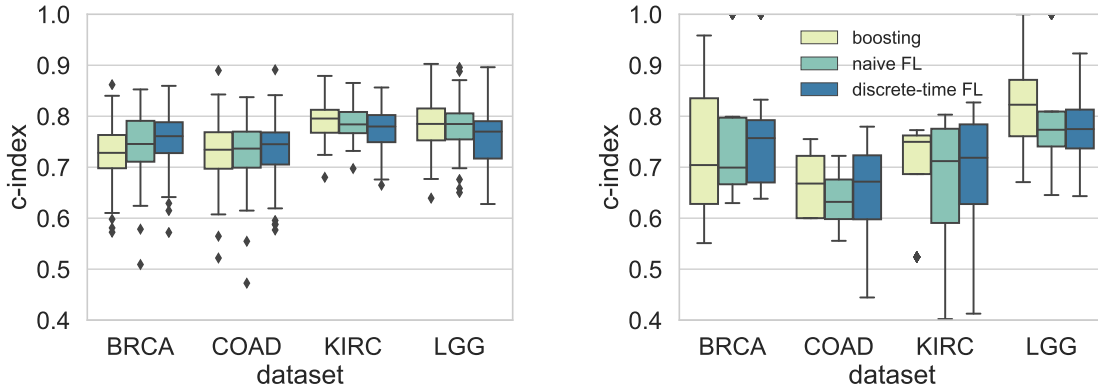


Figure 3: Experiments on 4 different TCGA tabular datasets, each spread across 4 to 6 centers depending on the dataset. Different approaches are compared, either using 5-fold cross validation with the test fold coming from the different centers (left), or in a out-of-center fashion, with the whole center data used for testing (right). Experiments do not reveal any significant difference in the performance of the different approaches, and discrete-time FL provides a reasonable performance in all cases.

Table 1: TCGA tabular datasets used in the experiments.

Cancer type	Number of patients $N$	Number of covariates $P$	Censoring percentage
BRCA	1096	41	86.2%
COAD	458	47	77.7%
KIRC	537	29	67.0%
LGG	514	20	75.7%

The TCGA patient’s barcode is used to identify unique patients and to map data collection to a specific tissue sort site (TSS). We identify 64 different sites, many of which contain very few samples. We thus regroup these sites in at most 6 different centers, corresponding to geographic regions: USA (Northeast, South, Midwest, West), Canada and Europe—countries from outside these regions do not have a significant amount of samples. Per-center details are provided in App. B.

For these 4 datasets, each split by the aforementioned centers, we evaluate the performance of 3 different schemes: boosting on the pooled data, naïve FL for minimizing the stratified Cox loss (4), and discrete-time FL (20) with  $\phi_\theta$  equal to identity. Cross-validation is performed in two different ways: either by 5-fold CV, with test folds coming from all centers (Fig. 3, left); or in an out-of-center fashion, with the whole center data used for testing (Fig. 3, right). Experiments do not reveal significant differences between approaches, and discrete-time FL provides reasonable performances in all cases.

### 6.3 Experiments on TCGA histopathology datasets

Finally, we demonstrate how this approach can be used also with more complex data and models by training a deep learning model on the digitally scanned histopathology slides that accompany the TCGA tabular data. We use the same datasets as in the previous subsection, up to small variations due to the absence of slides for some patients.

Histopathology slide images are very large in size, with up to  $10^5 \times 10^5$  pixels. We preprocess them with a standard pipeline [10, 7], first extracting matter-bearing, non-overlapping tiles from these images, then passing these tiles through an ImageNet-pretrained ResNet-50, and finally linearly autoencoding the penultimate ResNet layer’s output in order to decrease the number of features. Each slide thus results in an array of size  $8000 \times 256$ , where 8000 is the number of tiles extracted from the slide, and 256 the number of features per tile.

For the function  $\phi_\theta(\mathbf{x}_i)$ , we use a sequence of two 1D  $1 \times 1$  convolutions separated by a leaky ReLU, with the output of the second convolution being averaged over all dimensions. Similar architectures have been used in order to analyze histopathology data [10, 7]. The baseline is provided by training this exact same model on pooled data, but with a Cox loss instead, i.e. the *minibatch* method previously introduced. For clarity and due to the size of the dataset, we do not consider the pooled, local and ensemble baselines. Experimental details on datasets, preprocessing, and networks used can be found in App. C.

Table 2: C-index obtained on TCGA histopathology slides by both the discrete-time FL approach and the pooled baseline. Shown are mean and standard deviation over 5 runs of 5-fold CV.

Cancer type	MINI	DT-FL
BRCA	$0.55 \pm 0.06$	$0.57 \pm 0.06$
COAD	$0.62 \pm 0.07$	$0.65 \pm 0.07$
KIRC	$0.66 \pm 0.05$	$0.69 \pm 0.04$
LGG	$0.67 \pm 0.05$	$0.68 \pm 0.06$

Tab. 2 shows that, when applied to training state-of-the-art deep neural networks, discrete-time FL yields similar performance to minibatch optimization on pooled data. We note that for the COAD and KIRC cancer types discrete-time FL even slightly outperforms the baseline. Yet, this difference is not always significant, notably for the BRCA and LGG cancer types. We suspect that this slight improvement results from the difference between underlying models, which are only asymptotically equivalent, and, in particular, from the regularization introduced by the time-to-event quantization.

## 7 Conclusion

This paper investigates training survival models in a federated setting. Our results show that naïvely federating a Cox PH model amounts to training a stratified Cox PH model, which can have adverse effects of performance if done unchecked. Our proposed approach builds upon a discrete-time Cox model trained by stacking, which gives the same results in both federated and pooled settings. This approach compares favorably to previous works in terms of communication efficiency,

generality and privacy.

This paper opens many future research directions. Since the proposed model can be directly cast in federated learning frameworks, it is natural to study the impact of privacy-preserving techniques, such as differential privacy, on the performance of the resulting models. Similarly, one could study the impact of gradient compression techniques to further improve its communication efficiency.

## Acknowledgments

We would like to thank Flix Balazard for pointing out the connection between the naïve FL approach and the stratified Cox model. We also appreciate all the relevant feedback and comments from Owkin’s Lab, in particular from Michael Blum, Pierre Courtiol, Eric Tramel and Mikhail Zaslavskiy.

The results shown in this paper are in whole or part based upon data generated by the TCGA Research Network: <https://www.cancer.gov/tcga>.

## References

- [1] Martín Abadi, Ashish Agarwal, Paul Barham, Eugene Brevdo, Zhifeng Chen, Craig Citro, Greg S. Corrado, Andy Davis, Jeffrey Dean, Matthieu Devin, Sanjay Ghemawat, Ian Goodfellow, Andrew Harp, Geoffrey Irving, Michael Isard, Jia Yangqing, Rafal Jozefowicz, Lukasz Kaiser, Manjunath Kudlur, Josh Levenberg, Dandelion Mané, Rajat Monga, Sherry Moore, Derek Murray, Chris Olah, Mike Schuster, Jonathon Shlens, Benoit Steiner, Ilya Sutskever, Kunal Talwar, Paul Tucker, Vincent Vanhoucke, Vijay Vasudevan, Fernanda Viégas, Oriol Vinyals, Pete Warden, Martin Wattenberg, Martin Wicke, Yuan Yu, and Xiaoqiang Zheng. TensorFlow: Large-scale machine learning on heterogeneous systems, 2015. Software available from tensorflow.org.
- [2] Martin Abadi, Andy Chu, Ian Goodfellow, H Brendan McMahan, Ilya Mironov, Kunal Talwar, and Li Zhang. Deep learning with differential privacy. In *Proceedings of the 2016 ACM SIGSAC Conference on Computer and Communications Security*, pages 308–318. ACM, 2016.
- [3] Keith Bonawitz, Vladimir Ivanov, Ben Kreuter, Antonio Marcedone, H Brendan McMahan, Sarvar Patel, Daniel Ramage, Aaron Segal, and Karn Seth. Practical secure aggregation for privacy-preserving machine learning. In *Proceedings of the 2017 ACM SIGSAC Conference on Computer and Communications Security*, pages 1175–1191. ACM, 2017.
- [4] Paidamoyo Chapfuwa, Chenyang Tao, Chunyuan Li, Courtney Page, Benjamin Goldstein, Lawrence Carin, and Ricardo Henao. Adversarial time-to-event modeling. *arXiv preprint arXiv:1804.03184*, 2018.
- [5] Tianqi Chen and Carlos Guestrin. Xgboost: A scalable tree boosting system. In *Proceedings of the 22nd ACM SIGKDD International Conference on Knowledge Discovery and Data Mining*, pages 785–794. ACM, 2016.
- [6] Pierre Courtiol, Charles Maussion, Matahi Moarii, Elodie Pronier, Samuel Pilcer, Meriem Sefta, Pierre Manceron, Sylvain Toldo, Mikhail Zaslavskiy, Nolwenn Le Stang, et al. Deep learning-based classification of mesothelioma improves prediction of patient outcome. *Nature Medicine*, 25(10):1519–1525, 2019.

- [7] Pierre Courtiol, Eric W Tramel, Marc Sanselme, and Gilles Wainrib. Classification and disease localization in histopathology using only global labels: A weakly-supervised approach. *arXiv preprint arXiv:1802.02212*, 2018.
- [8] David R Cox. Regression models and life-tables. *Journal of the Royal Statistical Society: Series B (Methodological)*, 34(2):187–202, 1972.
- [9] Cameron Davidson-Pilon, Jonas Kalderstam, Paul Zivich, Ben Kuhn, Andrew Fiore-Gartland, AbdealiJK, Luis Moneda, Gabriel, Daniel Wilson, Alex Parij, Kyle Stark, Steven Anton, Lilian Besson, Jona, Harsh Gadgil, Dave Golland, Sean Hussey, Ravin Kumar, Javad Noorbakhsh, Andreas Klintberg, Dylan Albrecht, dhuynh, Dmitry Medvinsky, Denis Zgonjanin, Daniel S. Katz, Daniel Chen, Christopher Ahern, Chris Fournier, Arturo, and Andr F. Rendeiro. Cam-davidsonpilon/lifelines: v0.22.8, October 2019.
- [10] Thibaut Durand, Nicolas Thome, and Matthieu Cord. Weldon: Weakly supervised learning of deep convolutional neural networks. In *Proceedings of the IEEE Conference on Computer Vision and Pattern Recognition*, pages 4743–4752, 2016.
- [11] Cynthia Dwork, Aaron Roth, et al. The algorithmic foundations of differential privacy. *Foundations and Trends® in Theoretical Computer Science*, 9(3–4):211–407, 2014.
- [12] David V Glidden and Eric Vittinghoff. Modelling clustered survival data from multicentre clinical trials. *Statistics in Medicine*, 23(3):369–388, 2004.
- [13] JD Holt and RL Prentice. Survival analyses in twin studies and matched pair experiments. *Biometrika*, 61(1):17–30, 1974.
- [14] Diederik P. Kingma and Jimmy Ba. Adam: A method for stochastic optimization, 2014.
- [15] David G Kleinbaum and Mitchel Klein. *Survival analysis*, volume 3. Springer, 2010.
- [16] Vladimir Kolesnikov, Ahmad-Reza Sadeghi, and Thomas Schneider. Improved garbled circuit building blocks and applications to auctions and computing minima. In Juan A. Garay, Atsuko Miyaji, and Akira Otsuka, editors, *Cryptology and Network Security*, pages 1–20, Berlin, Heidelberg, 2009. Springer Berlin Heidelberg.
- [17] Jianfang Liu, Tara Lichtenberg, Katherine A Hoadley, Laila M Poisson, Alexander J Lazar, Andrew D Cherniack, Albert J Kovatich, Christopher C Benz, Douglas A Levine, Adrian V Lee, et al. An integrated TCGA pan-cancer clinical data resource to drive high-quality survival outcome analytics. *Cell*, 173(2):400–416, 2018.
- [18] Chia-Lun Lu, Shuang Wang, Zhanglong Ji, Yuan Wu, Li Xiong, Xiaoqian Jiang, and Lucila Ohno-Machado. WebDISCO: a web service for distributed Cox model learning without patient-level data sharing. *Journal of the American Medical Informatics Association*, 22(6):1212–1219, 2015.
- [19] Brendan McMahan, Eider Moore, Daniel Ramage, Seth Hampson, and Blaise Aguera y Arcas. Communication-efficient learning of deep networks from decentralized data. In *Proceedings of the 20th International Conference on Artificial Intelligence and Statistics (AISTATS)*, volume 54, pages 1273–1282. JMLR, 2017.

- [20] Xenia Miscouridou, Adler Perotte, Noémie Elhadad, and Rajesh Ranganath. Deep survival analysis: Nonparametrics and missingness. In *Machine Learning for Healthcare Conference*, pages 244–256, 2018.
- [21] Adam Paszke, Sam Gross, Francisco Massa, Adam Lerer, James Bradbury, Gregory Chanan, Trevor Killeen, Zeming Lin, Natalia Gimelshein, Luca Antiga, Alban Desmaison, Andreas Kopf, Edward Yang, Zachary DeVito, Martin Raison, Alykhan Tejani, Sasank Chilamkurthy, Benoit Steiner, Lu Fang, Junjie Bai, and Soumith Chintala. Pytorch: An imperative style, high-performance deep learning library. In *Advances in Neural Information Processing Systems 32*, pages 8024–8035. Curran Associates, Inc., 2019.
- [22] Rajesh Ranganath, Adler Perotte, Noémie Elhadad, and David Blei. Deep survival analysis. *arXiv preprint arXiv:1608.02158*, 2016.
- [23] G Rodriguez. Lecture notes for WWS509: Generalized linear statistical models. Princeton University, 2016.
- [24] Olaf Ronneberger, Philipp Fischer, and Thomas Brox. U-net: Convolutional networks for biomedical image segmentation. In Nassir Navab, Joachim Hornegger, William M. Wells, and Alejandro F. Frangi, editors, *Medical Image Computing and Computer-Assisted Intervention – MICCAI 2015*, pages 234–241, Cham, 2015. Springer International Publishing.
- [25] Felix Sattler, Simon Wiedemann, Klaus-Robert Müller, and Wojciech Samek. Sparse binary compression: Towards distributed deep learning with minimal communication. In *2019 International Joint Conference on Neural Networks (IJCNN)*, pages 1–8. IEEE, 2019.
- [26] Reza Shokri and Vitaly Shmatikov. Privacy-preserving deep learning. In *Proceedings of the 22nd ACM SIGSAC conference on computer and communications security*, pages 1310–1321. ACM, 2015.
- [27] Ping Wang, Yan Li, and Chandan K Reddy. Machine learning for survival analysis: A survey. *ACM Computing Surveys (CSUR)*, 51(6):1–36, 2019.
- [28] Yeming Wang, Dingyu Zhang, Guanhua Du, Ronghui Du, Jianping Zhao, Yang Jin, Shouzhi Fu, Ling Gao, Zhenshun Cheng, Qiaofa Lu, et al. Remdesivir in adults with severe covid-19: a randomised, double-blind, placebo-controlled, multicentre trial. *The Lancet*, 2020.
- [29] Lee-Jen Wei. The accelerated failure time model: a useful alternative to the cox regression model in survival analysis. *Statistics in medicine*, 11(14-15):1871–1879, 1992.
- [30] Peter WF Wilson, Ralph D’Agostino Sr, Deepak L Bhatt, Kim Eagle, Michael J Pencina, Sidney C Smith, Mark J Alberts, Jean Dallongeville, Shinya Goto, Alan T Hirsch, et al. An international model to predict recurrent cardiovascular disease. *The American Journal of Medicine*, 125(7):695–703, 2012.
- [31] Yue Zhao, Meng Li, Liangzhen Lai, Naveen Suda, Damon Civin, and Vikas Chandra. Federated learning with non-iid data. *arXiv preprint arXiv:1806.00582*, 2018.
- [32] Chenyang Zhong and Robert Tibshirani. Survival analysis as a classification problem. *arXiv preprint arXiv:1909.11171*, 2019.

- [33] Ligeng Zhu, Zhijian Liu, and Song Han. Deep leakage from gradients. In *Advances in Neural Information Processing Systems (NeurIPS) 32*, pages 14747–14756. Curran Associates, Inc., 2019.

## A Link between continuous-time and discrete-time models

We now explain how discrete-time models like (18) approximate the continuous-time Cox model (2), following the arguments of [32].

The contribution to the loss of an event happening to individual  $i$  at time  $t_i = s^{(m)}$  is

$$\alpha^{(m)} + \beta^T \phi_\theta(\mathbf{x}_i) - \sum_{j:t_j \geq t_i} \log(1 + e^{\alpha^{(m)} + \beta^T \phi_\theta(\mathbf{x}_j)}). \quad (22)$$

Optimizing over  $\alpha^{(m)}$  gives

$$\alpha_*^{(m)} = -\log \sum_j \frac{e^{\beta^T \phi_\theta(\mathbf{x}_j)}}{1 + e^{\alpha_*^{(m)} + \beta^T \phi_\theta(\mathbf{x}_j)}}. \quad (23)$$

If one assumes  $\alpha_*^{(m)} + \beta^T \phi_\theta(\mathbf{x}_j)$  to be very negative, then  $1 + e^{\alpha_*^{(m)} + \beta^T \phi_\theta(\mathbf{x}_j)} \approx 1$ , and  $\alpha_*^{(m)} \approx -\log \sum_j e^{\beta^T \phi_\theta(\mathbf{x}_j)}$ . Replacing this expression in (22) while setting  $\phi_\theta$  to the identity function shows the contribution of each event is effectively the same as that of the Cox loss (3).

## B Datasets from The Cancer Genome Atlas

We provide additional details on the datasets extracted from The Cancer Genome Atlas (TCGA). We distinguish between the tabular and image data as both datasets do not overlap entirely, and yield slightly different counts. These variations do not exceed 5% in the total number of patients in any cancer dataset.

Centers correspond to geographic regions obtained by looking up at TCGA metadata [17]. We restrict ourselves to 6 geographic regions, 4 of them belonging to the USA (Northeast, South, West, and Middlewest), 1 for Europe, and 1 for Canada, and ignore the remaining ones as they do not bring enough patients.

For both image and tabular data, we use the same event times for each relevant patient, and restrict ourselves to centers for which data points are available. Further, we remove centers for which only a single entry is available, as it prevents one from carrying out any meaningful intra-center cross-validation. As a consequence, depending on the cancer dataset, the number of centers varies between 3 and 6.

Figs. 4 and 5 show the details of the data distributions for tabular and image data, respectively.

## C Experimental details

In all experiments, c-indices of the proposed discrete-time method are computed on the true times  $t_i$  and not the binned ones, which are only used for training. This ensures a fair comparison of the c-indices of all reported approaches. Further, in all cases, hyperparameters were manually tuned, following a limited number of cross-validation runs.

### C.1 Section 6.1

For pooled, local and ensembled baselines, the `lifelines` class `CoxPHFitter` is used for fitting a Cox model with all default parameters, in particular with no regularization. The version of `lifelines` [9] used is 0.22.8.

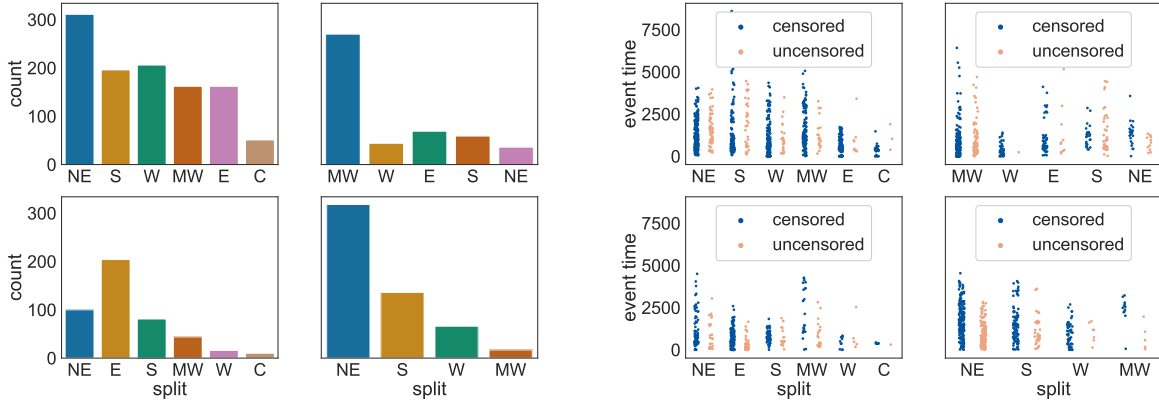


Figure 4: Details on the tabular datasets from TCGA. In each figure, from left to right and top to bottom, the cancer types are BRCA, LGG, COAD and KIRC. *Left*: Number of patients per center. *Right*: Distribution of event times per center. NE, S, W, MW, E, C respectively stand for Northeast, South, West, Midwest, Europe and Canada.

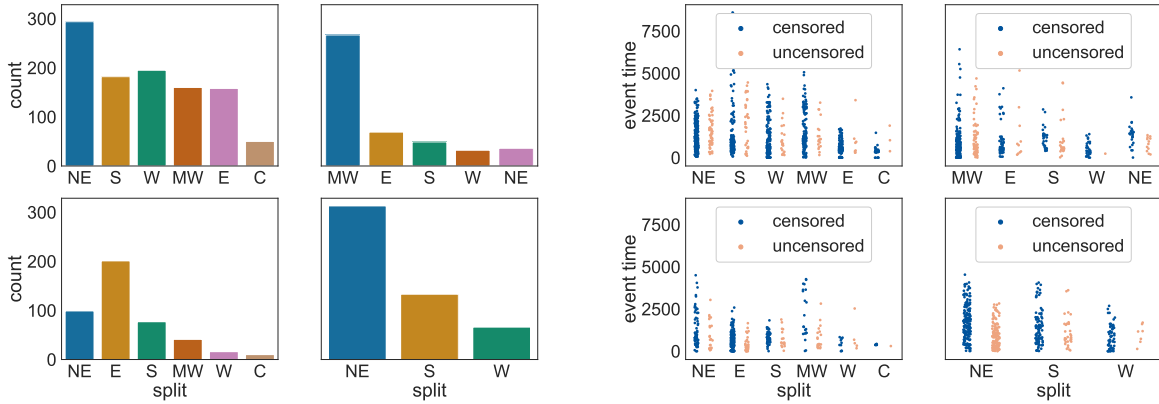


Figure 5: Details on the histopathology datasets from TCGA. In each figure, from left to right and top to bottom, the cancer types are BRCA, LGG, COAD and KIRC. *Left*: Number of patients per center. *Right*: Distribution of event times per center. NE, S, W, MW, E, C respectively stand for Northeast, South, West, Midwest, Europe and Canada.

Both minibatch and naive FL experiments are implemented using PyTorch [21] (version 1.14.0), with the Cox loss optimization performed using Adam [14] with a learning rate of  $10^{-3}$ . Batches are sampled with replacement; in total 5000 batches of size 100 each are used. For the naive FL experiments, we simulate the existence of multiple clients by looping through centers and storing the produced gradients; once all clients have been seen, these stored gradients are aggregated, and the aggregate used by the optimizer.

The exact same parameters are used to minimize the BCE loss in the case of discrete-time FL. Discrete times are created using  $Q = 1$ , so that all unique event times are considered.

## C.2 Section 6.2

For boosting, hyperparameters such as the learning rate (`eta`), the maximum depth of a tree (`max_depth`) and the subsample ratio (`subsample`) are fixed to respectively 0.01, 3, 0.5, reasonable values working generally well on such tabular data. The optimal number of boosting rounds is set using an inner 5-fold cross-validation on the training set. The version of `xgboost` [5] used is 0.90.

For naive FL, the same parameters as in Section 6.1 are used. For discrete-time FL, samples are created using  $Q = 30$  (i.e. binning events by month), and 1000 batches of size 5000 are used. Moreover, a weighted BCE loss is used such that positive samples are given more importance, following the ratio between negative and positive samples.

## C.3 Section 6.3

### C.3.1 Slide preprocessing

**Tile extraction** We first extract matter-bearing, non-overlapping tiles from each histopathology slide. For this purpose, a single U-Net [24] is trained to separate all individual pixels between foreground (containing matter) and background, using manually annotated tiles of histology images. Using this U-Net, we extract 8000 tiles per slide.

**ResNet feature extraction** Each extracted tile is processed through an ImageNet-pretrained ResNet-50 deep neural network, stopping at the penultimate layer of the architecture (before getting logits), leading to a vector of size 2048 per tile.

**Dimensionality reduction** At this stage of preprocessing, each slide has been transformed into an array of size  $8000 \times 2048$ , where 8000 is the number of tiles extracted from the slide and 2048 the number of features per tile. Due to this large dimensionality and the few number of samples, to reduce overfitting, we additionally perform a feature reduction operation. For each cancer’s dataset, we train a linear autoencoder on ResNet features of tiles extracted from this dataset, with bottleneck dimension 256 and no bias. This autoencoder is trained for the reconstruction of the original tiles’ features under the Mean-Square Error loss. This training is carried out using the Adam optimizer with standard hyperparameters and learning rate  $10^{-3}$  on a subset of 100,000 randomly-sampled tiles for 3 epochs.

**Final representation** After passing each tile’s ResNet features through the encoder part of the trained autoencoder, each individual slide is finally represented by an array of shape  $8000 \times 256$ , which concludes preprocessing.

### C.3.2 Network architectures and training

We first describe settings common to the baseline and discrete-time FL approaches.

**Cross-validation** We perform 5 runs of 5-fold cross-validation, each initialized with a different seed. In each CV, the validation sets are built from the local centers’ validation set. In both cases, cross validation is done with a patient split. In particular, during evaluation, patients with multiple slides have the scores for each slide averaged, yielding a single score per patient. In the training folds, all slides belonging to a center are treated as independent samples.

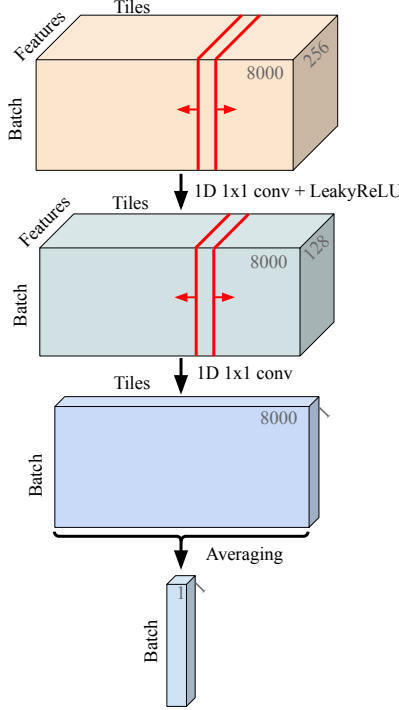


Figure 6: Auxiliary model  $\phi_\theta$  applied to preprocessed histopathology slide images. The use of 1D  $1 \times 1$  convolutions ensures that the same layer is applied to all tiles of a given slide. The batch axis corresponds to multiple slides. The negative slope of the LeakyReLU is set to 0.1.

**Auxiliary model** The same auxiliary model, *i.e.* the function  $\phi_\theta$ , is the same in both approaches. Its architecture is depicted in Figure 6 and begins with a 1D  $1 \times 1$  convolution of output size 128, a Leaky ReLU with negative slope of 0.1, and another 1D  $1 \times 1$  convolution of output size 1. Due to the use of  $1 \times 1$  convolutions, each tile is assigned a single scalar score by a shared network. Then, the average of all scores across tiles is computed, leading to a single score per slide, which is the output of the auxiliary model.

**Baseline training** The baseline (MINI) experiments are carried out with Tensorflow [1] (version 1.14). The network training uses the following hyperparameters: batch size 30, 20 epochs, optimizer Adam with learning rate set to  $10^{-3}$  and standard hyperparameters otherwise.

**Discrete-time FL training** For discrete-time FL, experiments are carried with PyTorch (version 1.14.0). Batches of size 100 are sampled without replacement, totalling 25 epochs. The optimizer Adam is used, with learning rate set to  $10^{-3}$  and standard hyperparameters otherwise. Regarding the binning of times-to-event, once again,  $Q$  is set to 30 and label balancing is used in the BCE loss.